Cluster Compounds

International Edition: DOI: 10.1002/anie.201811331
German Edition: DOI: 10.1002/ange.201811331

Atomically Precise Expansion of Unsaturated Silicon Clusters

Kinga I. Leszczyńska, Volker Huch, Carsten Präsang, Jan Schwabedissen, Raphael J. F. Berger,* and David Scheschkewitz**

Dedicated to Professor Robert West on the occasion of his 90th birthday

Abstract: *Small- to medium-sized clusters occur in various areas of chemistry, for example, as active species of heterogeneous catalysis or as transient intermediates during chemical vapor deposition. The manipulation of stable representatives is mostly limited to the stabilizing ligand periphery, virtually excluding the systematic variation of the property-determining cluster scaffold. We now report the deliberate expansion of a stable unsaturated silicon cluster from six to seven and finally eight vertices. The consecutive application of lithium/naphthalene as the reducing agent and decamethylsilicocene as the electrophilic source of silicon results in the expansion of the core by precisely one atom with the potential of infinite repetition.*

Small- to medium-sized clusters assume key roles in various technologically important areas. In heterogeneous reactions, metal and metal compound clusters are powerful catalysts for chemical transformations on an industrial scale.[1] Metal and semi-metal clusters constitute key intermediates during the chemical vapor deposition of thin films and bulk[2] as well as during the bottom-up synthesis of nanoparticles.[3] Although a remarkable number of stable molecular clusters have been reported, for example, $Si_{32}R_{45}^-$,[4] $(CdSe)_{34}$,[5] $R_{20}Al_{77}^{2-}$,[6] and $R_{44}Au_{102}$[7] (R = ligand or functional group), they are typically obtained in a non-systematic or even serendipitous manner, often entailing difficulties with yield and reproducibility.

Unsaturated silicon clusters with partial substitution (siliconoids) have attracted attention for their role as proposed intermediates in gas-phase deposition processes. With their unsubstituted vertices, they share important surface features of both nanoparticles and the elemental bulk.[8] The preference of silicon for single bonds as opposed to the competitive strength of multiple bonds in the corresponding carbon systems leads to a growing dominance of cluster motifs when the number of silicon core atoms is increased.[9] For example, the first stable siliconoid, Si_5R_6[10a] (**1**; Scheme 1),

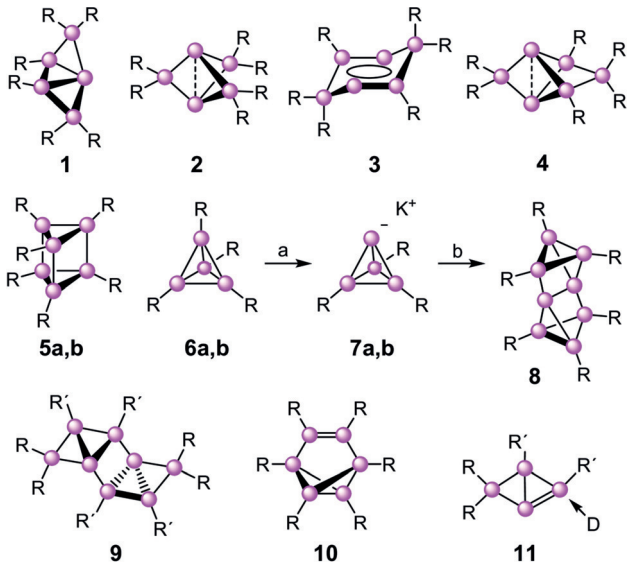

Scheme 1. Selected saturated and unsaturated silicon clusters. **1**, **3**, **4**, **5a**: R = Tip = 2,4,6-*i*Pr$_3$C$_6$H$_2$; **2**: R = 2,4,6-Me$_3$C$_6$H$_2$; **5b**: R = 2,6-*i*Pr$_2$C$_6$H$_3$; **6a**, **7a**, **8**: R = *t*Bu$_3$Si; **6b**, **7b**: R = ((Me$_3$Si)$_2$CH)$_2$(Me)Si; **9**, **11**: (R)$_2$ = C(SiMe$_3$)$_2$CH$_2$CH$_2$C(SiMe$_3$)$_2$, R′ = *t*Bu; **10**: (R)$_2$ = C(SiMe$_3$)$_2$C-(Me)$_2$C(SiMe$_3$)$_2$; **11**: D = *p*-(dimethylamino)pyridine. **a**: KC_8; **b**: ICl.

adopts a tricyclic framework with one unsubstituted silicon vertex, and the isomeric pentasilapropellane **2** even features two "naked" cluster atoms.[10b] The low-energy Si_6R_6 isomers **3**[10c] and **4**[10d] are both characterized by a cluster framework with two unsaturated vertices, in marked contrast to the iconic benzene, which is by far the lowest energy structure on the C_6H_6 potential energy surface.[11]

While solvated Zintl ions—charged, polyhedral clusters—of germanium and tin can be used as well-defined precursors for the synthesis of partially substituted molecular clusters,[12] the strongly reducing silicon congeners have only been employed as ligands towards a few redox-stable transition-metal fragments,[13] and were only very recently protonated to the partially hydrogen-substituted clusters $[HSi_9]^{3-}$ and $[H_2Si_9]^{2-}$.[14] Therefore, siliconoids are typically accessed by

[*] Dr. K. I. Leszczyńska, Dr. V. Huch, Dr. C. Präsang, Prof. Dr. D. Scheschkewitz
Krupp-Chair of Inorganic and General Chemistry
Saarland University
Campus Saarbrücken C41, 66123 Saarbrücken (Germany)
E-mail: kinga.leszczynska@uni-saarland.de
scheschkewitz@mx.uni-saarland.de
Dr. J. Schwabedissen, Dr. R. J. F. Berger
Division of Materials Chemistry, University of Salzburg
5020 Salzburg (Austria)
E-mail: raphael.berger@sbg.ac.at
Supporting information and the ORCID identification number(s) for the author(s) of this article can be found under: https://doi.org/10.1002/anie.201811331.

reductive cleavage of competent leaving groups from classical saturated precursors. This approach was initially demonstrated by the preparation of saturated polyhedral silicon clusters such as hexasilaprismane R_6Si_6 **5a**,**b**[15] and tetrasilatetrahedrane R_4Si_4 **6a**,**b**[16] by reductive dimerization of the corresponding linear $R_2Si_2X_4$ or cyclic $R_3Si_3X_3$ building blocks. Functionalization of the saturated Si_4 core was achieved with KC_8 to yield isolable tetrasilatetrahedranides $K^+[R_3Si_4^-]$ **7a**,**b**.[16b,c] Oxidation of **7a** with iodine monochloride gave siliconoid R_6Si_8 **8**,[17] which had previously been synthesized from a different R_3Si_4 precursor by reduction.[18] Further examples of isolable siliconoids were reported by Iwamoto[19] (**9**, **11**) and Kyushin[20] (**10**). Despite the isolated reports of core expansion of siliconoids,[15b,19] the number of atoms in the scaffold, once assembled, cannot be increased in a systematic way.

Based on our report on the first anionic siliconoid with partial substitution $Si_6R_5^-$ (**12**; R = Tip = 2,4,6-triisopropylphenyl),[21] we sought to develop an atomically precise cluster expansion procedure. As the leaving group properties of the pentamethylcyclopentadienyl ligand (Cp*) are well-established in main group chemistry,[22] we speculated that Jutzi's decamethylsilicocene ($SiCp^*_2$;[23] despite the decacoordinate silicon atom) might react with **12** as an electrophilic source of precisely one silicon atom. Previously, only the corresponding cation $Cp^*Si^+BAr_4^-$ (Ar = pentafluorophenyl)[24] had been employed as electrophile.[25] As proof of principle, we carried out the reaction of $R_2Si{=}Si(R)Li$ with $SiCp^*_2$. Indeed, the literature-known Cp*-substituted cyclotrisilene, *cyclo*-$Si_3Tip_3Cp^*$, was obtained in 90% yield (determined by NMR spectroscopy).[26]

More importantly, treatment of the anionic siliconoid **12** with one equivalent of $SiCp^*_2$ led to a uniform product **13** accompanied by precipitation of Cp*Li (Scheme 2). ^{1}H NMR analysis of **13** in C_6D_6 confirmed the presence of five nonequivalent Tip groups. The additional singlet resonance at 1.69 ppm corresponds to 15 hydrogen atoms and is assigned to the remaining Cp* substituent. The characteristic wide

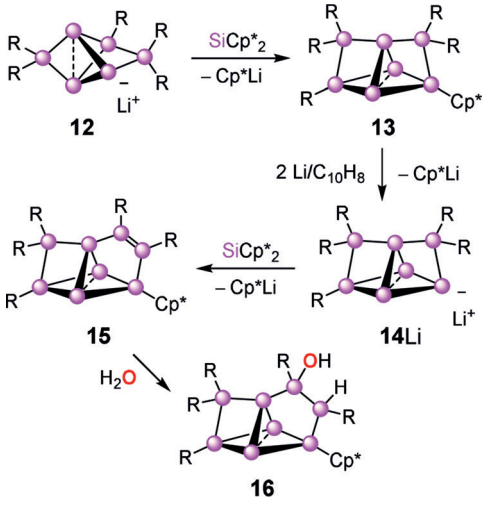

Scheme 2. Cluster expansion from the anionic Si_6 siliconoid **12** to the Si_7 siliconoids **13** and **14** and finally the Si_8 siliconoids **15** and **16**. R = Tip = 2,4,6-*i*$Pr_3C_6H_2$, Cp* = 1,2,3,4,5-pentamethylcyclopentadienyl.

distribution of ^{29}Si NMR chemical shifts of siliconoid **4** and its derivatives (typically from about −270 ppm for the "naked" vertices to +175 ppm for the adjacent R_2Si bridge)[8] was retained in the new product. A third strongly shielded resonance at −138.4 ppm without a cross-peak in the ^{29}Si–^{1}H correlation NMR spectrum suggested the presence of an additional silicon vertex without a substituent. As the predicted global-minimum isomer of the Si_7H_6 potential energy surface $\mathbf{13_H}$[27] has precisely three "naked" vertices, we calculated the ^{29}Si NMR spectrum of a B3LYP/def2-TZVP-optimized model system for **13** corresponding to the experimental case ($\mathbf{13_{Tip}}$) at the OLYP/def2-TZVP level of theory.[28] The excellent agreement of the calculated chemical shifts of $\mathbf{13_{Tip}}$ with those experimentally observed for **13** suggests very similar constitutions (Table 1; much less satisfactory agreement was achieved with the B3LYP functional; see Table S9, Supporting Information).

Table 1: Experimental (**13**, **14**·$Li^+(thf)_3$, **15**) and calculated ($\mathbf{13_{Tip}}$, $\mathbf{14_{Tip}}$·$Li^+(thf)_3$, $\mathbf{15_{Tip}}$) ^{29}Si NMR chemical shifts [ppm] at the OLYP/def2-TZVP level of theory. Atoms of **15** and $\mathbf{15_{Tip}}$ are numbered as in **16**.

	13	$\mathbf{13_{Tip}}$	14	$\mathbf{14_{Tip}}$	15	$\mathbf{15_{Tip}}$
Si1	−229.6	−237.6	−191.9	−197.0	−138.9	−151.9
Si2	−241.9	−255.5	−195.7	−204.8	−165.1	−160.5
Si3	181.9	180.3	284.3	292.1	18.7	5.9
Si4	2.6	10.6	10.8	18.1	33.5	41.0
Si5	−138.4	−139.4	−66.1	−73.1	−81.7	−82.2
Si6	15.0	20.2	60.1	78.4	111.8	115.5
Si7	156.0	154.6	148.0	150.7	60.3	80.2
Si8					206.9	201.0

The structure of siliconoid $Si_7R_5Cp^*$ in the solid state was finally confirmed as the first stable example of a neutral siliconoid with three adjacent unsubstituted vertices **13** by X-ray diffraction on orange-red crystals obtained in 53% yield (Figure 1).[29] The cluster scaffold is almost indistinguishable from that predicted for $\mathbf{13_H}$ and $\mathbf{13_{Tip}}$.[27] The three unsubstituted vertices form an isosceles triangle, with the base and apex bridged on both sides by electron-precise disilanyl units.

The Si1–Si2 distance of 264.8(1) pm is relatively long, while all Si–Si bonds of the cluster core (231.8–241.8 pm) show typical Si–Si single bond lengths. Alternatively, the Si7 scaffold of siliconoid **13** can be described as a persilapropellane with twofold R_2Si bridging of the propeller blades and an unprecedented seesaw-type tetracoordination of Si5 as shown by the close-to-linear bond angle Si4-Si5-Si6 of 173.88(4)°.

The remaining Cp* group in **13** should allow for the regeneration of the anionic functionality after the first core expansion step. The Si_7 siliconoid **13** was therefore treated with two equivalents of lithium/naphthalene in tetrahydrofuran (thf) at −100 °C in order to obtain the anion **14**. ^{1}H NMR spectroscopy of the uniform reaction mixture confirmed the presence of five Tip substituents, while the resonance of the Cp* group had indeed completely vanished. Instead, characteristic signals for three equivalents of coordinated thf suggested the incorporation of a lithium cation into the molecule. The ^{29}Si NMR spectrum exhibited a similar distribution of the seven signals as the starting material **13**.

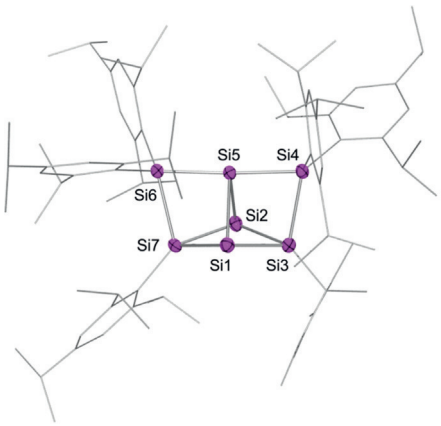

Figure 1. Molecular structure of siliconoid **13** in the solid state. Hydrogen atoms are omitted for clarity. Thermal ellipsoids set at 50% probability. Selected bond lengths [pm] and angles [°]: Si1–Si2 264.8(1), Si1–Si5 234.41(9), Si1–Si3 231.63(9), Si2–Si5 234.19(9), Si3–Si4 241.81(9), Si4–Si5 238.86(9), Si5–Si6 238.42(9), Si6–Si7 241.55(9); Si1-Si5-Si2 68.82(3), Si1-Si3-Si2 69.45(3), Si4-Si5-Si6 173.77(4).

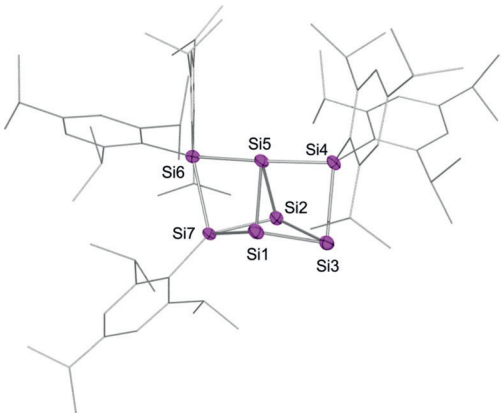

Figure 2. Molecular structure of the solvent-separated anionic siliconoid **14** in the solid state. Hydrogen atoms and the $[Li^+(dme)_3]$ countercation are omitted for clarity. Thermal ellipsoids set at 50% probability. Selected bond lengths [pm] and angles [°]: Si1–Si2 255.96(8), Si1–Si5 233.77(8), Si1–Si3 239.37(8), Si2–Si5 231.96(8), Si3–Si4 244.82(8), Si4–Si5 235.68(8), Si5–Si6 237.59(8), Si6–Si7 241.12(7); Si1-Si5-Si2 66.68(2), Si1-Si3-Si2 64.16(2), Si4-Si5-Si6 174.00(3).

The most remarkable difference is the downfield shift of the formerly Cp*-bonded silicon vertex by about $\Delta\delta = 100$ ppm, which was accompanied by substantial line broadening due to coupling to the quadrupolar ^{7}Li nucleus ($\delta(^7Li) = -0.15$ ppm). In contrast, the unsubstituted vertices are only shifted by $\Delta\delta = 40$ to 70 ppm. A similar relative deshielding had been observed between the neutral Si_6 siliconoid **4** and the corresponding lithiated species **12**.[21] Applying the OLYP functional, the calculated ^{29}Si chemical shifts of the B3LYP-optimized model $Tip_5Si_7(Li)thf_3$ (**14**$_{Tip}$·$Li^+(thf)_3$) nicely reproduce the experimental data of **14**·$Li^+(thf)_3$ (Table 1).

A crystalline sample of **14** was obtained from pentane in 42% yield. As shown by single-crystal X-ray diffraction, the lithiated siliconoid **14**·$Li^+(thf)_3$ crystallizes as a contact ion pair from pentane solution (see the Supporting Information). The structural parameters of the cluster scaffold of **14**·$Li^+(thf)_3$ are similar to those of the neutral precursor **13** except for the noticeably shortened base of the central triangle (Si1–Si2 = 254.48(5) pm; $\Delta = 10.3$ pm). In order to assess the influence of the close contact of the lithium cation to the anionic Si_7 siliconoid, the solvent-separated ion pair **14**$[Li^+(dme)_3]$ was prepared by crystallization from a mixture of hexane and 1,2-dimethoxyethane in 73% yield. Except for significant sharpening of the ^{29}Si NMR resonance of Si3 due to the absence of a direct interaction with the quadrupolar ^{7}Li nucleus, all other resonances remained essentially unchanged. Similarly, the solid-state structure of **14**$[Li^+(dme)_3]$ is hardly influenced by the spatially distant Li^+ countercation (Figure 2).

With anionic siliconoid **14** in hand, the obvious next step was the incorporation of an eighth silicon vertex. Similar to the synthesis of neutral Si_7 cluster **13** from anionic **12**, the reaction of **14** with $SiCp^*_2$ yielded a uniform product **15** (90% spectroscopic purity). In this case, the observation of only three of the eight resonances at high field ($\delta = -165.1$, -138.9, -81.7 ppm) suggested the migration of an aryl group from a disubstituted SiR_2 unit to a formerly "naked" vertex. Indeed, a ^{1}H–^{29}Si correlation spectrum revealed only one SiR_2 unit ($\delta = 33.5$ ppm), while four resonances ($\delta = 111.8$, 60.3, 35.5, 18.7 ppm) are due to SiR vertices bonded to just one substituent.

In one crystallization attempt, a few orange single crystals were collected and then investigated by X-ray diffraction (Figure 3). Instead of the $Si_8R_5Cp^*$ siliconoid **15**, however, its water adduct **16** with a central unit of three unsubstituted silicon atoms was obtained. The formerly almost linear bond angle of the Si_7 siliconoids **13** and **14** at Si5 is with 149.53(5)° much more acute in **16**. Apparently, the release of strain results in an approximation of regular tetrahedral coordination at Si5.

The deliberate addition of one equivalent of H_2O to **15** led to the near quantitative formation of **16** (85% spectroscopic

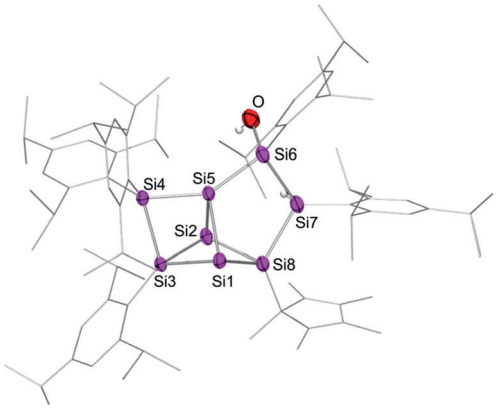

Figure 3. Molecular structure of siliconoid **16** in the solid state. Hydrogen atoms (except OH and SiH) and co-crystallized solvent molecules are omitted for clarity. Thermal ellipsoids set at 50% probability. Selected bond lengths [pm] and angles [°]: Si1–Si2 263.8(1), Si1–Si5 234.2(1), Si1–Si8 235.70(13), Si2–Si5 233.97(13), Si2–Si8 232.7(1), Si7–Si8 236.9(1), Si6–Si7 237.6(1), Si5–Si6 232.3(1), Si6–O 169.0(3); Si1-Si5-Si2 68.60(4), Si4-Si5-Si6 149.53(5).

yield). Using the structure of **16** (minus H_2O) as a reasonable starting point, we optimized the geometry of $\mathbf{15_{Tip}}$ at the B3LYP/def2-TZVP level of theory. The resulting R_6Si_8 cluster is related to the Si_7 species **13** inasmuch as one of the SiR_2 moieties is formally replaced by an exohedral unsaturated Si=Si bridge (Si6 and Si7). The calculated HOMO and LUMO of **15** are predominantly constituted by the π and π* components at this Si=Si moiety, which readily explains the selective H_2O addition across this bond (Figure 4). The

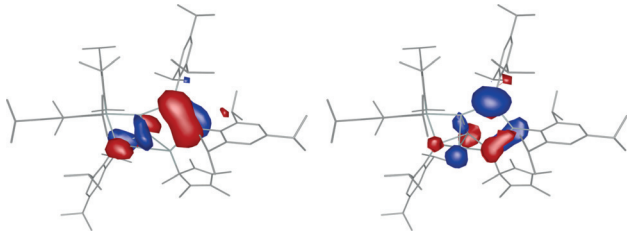

Figure 4. Calculated HOMO (left) and LUMO (right) of Si_8 siliconoid $\mathbf{15_{Tip}}$.

experimental ^{29}Si NMR signals of **15** at $\delta = 111.8$ (Si6) and 60.3 ppm (Si7) can be assigned to the exohedral Si=Si unit on the basis of their similarity to those reported for 1,2-disilyl-1,2-diaryl disilenes with chemical shifts between 85 and 130 ppm.[30] Unsymmetrical substitution is well-known to lead to polarized Si=Si bonds with sometimes extremely differing chemical shifts for the tricoordinate Si atoms.[31] All calculated ^{29}Si chemical shifts of $\mathbf{15_{Tip}}$ (obtained with the OLYP functional) show a convincing agreement with the experimental data. Those of the exohedral Si=Si moiety at $\delta = 115.5$ (Si6) and 80.2 ppm (Si7) are (as usually observed for atoms with bonding including a pronounced π-component) slightly overestimated, but otherwise nicely reproduce this trend (Table 1). Indeed, the calculated structure of $\mathbf{15_{Tip}}$ confirms appreciable pyramidalization at the relatively upfield-shifted silicon atom Si7 with a sum of bond angles of $\Sigma = 333.4°$, while the downfield-shifted silicon atom Si6 is much closer to planarity ($\Sigma = 358.1°$). Consistent with the electrophilic nature of Si6 in **15**, the OH group is attached to the corresponding atom of the hydrolysis product **16**.

In conclusion, with the systematic transformation of the anionic Si_6 siliconoid **12** (R = Tip) into species with seven and even eight vertices **13**, **14**, and **15**, we have provided proof-of-concept results for the stepwise and repeated expansion of clusters with atomic precision. Key to this method is the use of decamethylsilicocene as an electrophilic source of divalent silicon with pentamethylcyclopentadienide ligands (Cp*) as anionic leaving groups. As our process allows for the regeneration of the anionic functionality after the expansion step, a rapid increase in the number of available siliconoids (including heteroatom-doped variants) can be expected. The ubiquitous use of Cp* throughout the Periodic Table may allow for application well beyond the realm of silicon clusters.

Acknowledgements

This work was supported by the Deutsche Forschungsgemeinschaft (DFG SCHE906/4-1 and 4-2) and COST (Action CM1302). We thank Susanne Harling for elemental analysis and the reviewers whose comments contributed significantly to the improvement of the computational results. J.S. acknowledges the generous provision of computational resources by the Paderborn Center for Parallel Computing (PC^2).

Conflict of interest

The authors declare no conflict of interest.

Keywords: anions · cluster compounds · main group elements · silicon · subvalent compounds

How to cite: *Angew. Chem. Int. Ed.* **2019**, *58*, 5124–5128
Angew. Chem. **2019**, *131*, 5178–5182

[1] P. Munnik, P. E. de Jongh, K. P. de Jong, *Chem. Rev.* **2015**, *115*, 6687–6718.
[2] C. Hollenstein, *Plasma Phys. Controlled Fusion* **2000**, *42*, R93–R104.
[3] N. T. K. Thanh, N. Maclean, S. Mahiddine, *Chem. Rev.* **2014**, *114*, 7610–7630.
[4] J. Tillmann, J. H. Wender, U. Bahr, M. Bolte, H.-W. Lerner, M. C. Holthausen, M. Wagner, *Angew. Chem. Int. Ed.* **2015**, *54*, 5429–5433; *Angew. Chem.* **2015**, *127*, 5519–5523.
[5] Y. Wang, Y. Zhang, F. Wang, D. E. Giblin, J. Hoy, H. W. Rohrs, R. A. Loomis, W. E. Buhro, *Chem. Mater.* **2014**, *26*, 2233–2243.
[6] A. Ecker, E. Weckert, H. Schnöckel, *Nature* **1997**, *387*, 379–381.
[7] a) P. D. Jadzinsky, G. Calero, C. J. Ackerson, D. A. Bushnell, R. D. Kornberg, *Science* **2007**, *318*, 430–433; b) R. Rongchao, C. Zeng, M. Zhou, Y. Chen, *Chem. Rev.* **2016**, *116*, 10346–10413.
[8] Y. Heider, D. Scheschkewitz, *Dalton Trans.* **2018**, *47*, 7104–7112.
[9] A. S. Ivanov, A. I. Boldyrev, *J. Phys. Chem. A* **2012**, *116*, 9591–9598.
[10] a) D. Scheschkewitz, *Angew. Chem. Int. Ed.* **2005**, *44*, 2954–2956; *Angew. Chem.* **2005**, *117*, 3014–3016; b) D. Nied, R. Köppe, W. Klopper, H. Schnöckel, F. Breher, *J. Am. Chem. Soc.* **2010**, *132*, 10264–10265; c) K. Abersfelder, A. J. P. White, H. S. Rzepa, D. Scheschkewitz, *Science* **2010**, *327*, 564–566; d) K. Abersfelder, A. J. P. White, R. J. F. Berger, H. S. Rzepa, D. Scheschkewitz, *Angew. Chem. Int. Ed.* **2011**, *50*, 7936–7939; *Angew. Chem.* **2011**, *123*, 8082–8086.
[11] T. C. Dinadayalane, U. D. Priyakumar, G. N. Sastry, *J. Phys. Chem. A* **2004**, *108*, 11433–11448.
[12] a) S. Scharfe, F. Kraus, S. Stegmaier, A. Schier, T. F. Fässler, *Angew. Chem. Int. Ed.* **2011**, *50*, 3630–3670; *Angew. Chem.* **2011**, *123*, 3712–3754; b) S. C. Sevov, J. M. Goicoechea, *Organometallics* **2006**, *25*, 5678–5692; c) F. Li, A. Muñoz-Castro, S. C. Sevov, *Angew. Chem. Int. Ed.* **2012**, *51*, 8581–8584; *Angew. Chem.* **2012**, *124*, 8709–8712; d) F. Li, S. C. Sevov, *J. Am. Chem. Soc.* **2014**, *136*, 12056–12063; e) F. S. Geitner, J. V. Dums, T. F. Fässler, *J. Am. Chem. Soc.* **2017**, *139*, 11933–11940; f) F. S. Geitner, W. Klein, T. F. Fässler, *Angew. Chem. Int. Ed.* **2018**, *57*, 14509–14513; *Angew. Chem.* **2018**, *130*, 14717–14721; g) S. Frischhut, W. Klein, M. Drees, T. F. Fässler, *Chem. Eur. J.* **2018**, *24*, 9009–9014; h) O. Kysliak, C. Schrenk, A. Schnepf, *Inorg. Chem.* **2015**, *54*, 7083–7088; i) O. Kysliak, A. Schnepf, *Dalton Trans.* **2016**, *45*, 2404–2408.

[13] a) S. Joseph, M. Hamberger, F. Mutzbauer, O. Härtl, M. Meier, N. Korber, *Angew. Chem. Int. Ed.* **2009**, *48*, 8770 – 8772; *Angew. Chem.* **2009**, *121*, 8926 – 8929; b) M. Waibel, F. Kraus, S. Scharfe, B. Wahl, T. F. Fässler, *Angew. Chem. Int. Ed.* **2010**, *49*, 6611 – 6615; *Angew. Chem.* **2010**, *122*, 6761 – 6765.

[14] a) T. Henneberger, W. Klein, T. F. Fässler, *Z. Anorg. Allg. Chem.* **2018**, *644*, 1018 – 1027; b) C. Lorenz, F. Hastreiter, J. Hioe, N. Lokesh, S. Gärtner, N. Korber, R. M. Gschwind, *Angew. Chem. Int. Ed.* **2018**, *57*, 12956 – 12960; *Angew. Chem.* **2018**, *130*, 13138 – 13142; c) L. J. Schiegerl, A. J. Karttunen, J. Tillmann, S. Geier, G. Raudaschl-Sieber, M. Waibel, T. F. Fässler, *Angew. Chem. Int. Ed.* **2018**, *57*, 12950 – 12955; *Angew. Chem.* **2018**, *130*, 13132 – 13137.

[15] a) A. Sekiguchi, T. Yatabe, C. Kabuto, H. Sakurai, *J. Am. Chem. Soc.* **1993**, *115*, 5853 – 5854; b) K. Abersfelder, A. Russell, H. S. Rzepa, A. J. P. White, P. R. Haycock, D. Scheschkewitz, *J. Am. Chem. Soc.* **2012**, *134*, 16008 – 16016.

[16] a) N. Wiberg, C. M. M. Finger, K. Polborn, *Angew. Chem. Int. Ed. Engl.* **1993**, *32*, 1054 – 1056; *Angew. Chem.* **1993**, *105*, 1140 – 1142; b) M. Ichinohe, M. Toyoshima, R. Kinjo, A. Sekiguchi, *J. Am. Chem. Soc.* **2003**, *125*, 13328 – 13329; c) T. M. Klapötke, S. K. Vasisht, G. Fischer, P. Mayer, *J. Organomet. Chem.* **2010**, *695*, 667 – 672.

[17] N. Wiberg, S.-K. Vasisht, G. Fischer, P. Mayer, V. Huch, M. Veith, *Z. Anorg. Allg. Chem.* **2007**, *633*, 2425 – 2430.

[18] G. Fischer, V. Huch, P. Mayer, S. K. Vasisht, M. Veith, N. Wiberg, *Angew. Chem. Int. Ed.* **2005**, *44*, 7884 – 7887; *Angew. Chem.* **2005**, *117*, 8096 – 8099.

[19] T. Iwamoto, N. Akasaka, S. Ishida, *Nat. Commun.* **2014**, *5*, 5353.

[20] a) A. Tsurusaki, C. Iizuka, K. Otsuka, S. Kyushin, *J. Am. Chem. Soc.* **2013**, *135*, 16340 – 16343; b) S. Ishida, K. Otsuka, Y. Toma, S. Kyushin, *Angew. Chem. Int. Ed.* **2013**, *52*, 2507 – 2510; *Angew. Chem.* **2013**, *125*, 2567 – 2570.

[21] P. Willmes, K. Leszczyńska, Y. Heider, K. Abersfelder, M. Zimmer, V. Huch, D. Scheschkewitz, *Angew. Chem. Int. Ed.* **2016**, *55*, 2907 – 2910; *Angew. Chem.* **2016**, *128*, 2959 – 2963.

[22] P. Jutzi, G. Reumann, *J. Chem. Soc. Dalton Trans.* **2000**, 2237 – 2244.

[23] P. Jutzi, D. Kanne, C. Krüger, *Angew. Chem. Int. Ed. Engl.* **1986**, *25*, 164 – 164; *Angew. Chem.* **1986**, *98*, 163 – 164.

[24] P. Jutzi, A. Mix, B. Rummel, W. W. Schoeller, B. Neumann, H.-G. Stammler, *Science* **2004**, *305*, 849 – 851.

[25] a) P. Jutzi, *Chem. Eur. J.* **2014**, *20*, 9192 – 9207; b) P. Jutzi, K. Leszczyńska, A. Mix, B. Neumann, B. Rummel, W. Schoeller, H.-G. Stammler, *Organometallics* **2010**, *29*, 4759 – 4761; c) S. Inoue, K. Leszczyńska, *Angew. Chem. Int. Ed.* **2012**, *51*, 8589 – 8593; *Angew. Chem.* **2012**, *124*, 8717 – 8721; d) K. Leszczyńska, K. Abersfelder, M. Majumdar, B. Neumann, H.-G. Stammler, H. S. Rzepa, P. Jutzi, D. Scheschkewitz, *Chem. Commun.* **2012**, *48*, 7820 – 7822; e) P. Ghana, M. I. Arz, G. Schnakenburg, M. Straßmann, A. C. Filippou, *Organometallics* **2017**, *37*, 772 – 780.

[26] K. Leszczyńska, K. Abersfelder, A. Mix, B. Neumann, H.-G. Stammler, M. J. Cowley, P. Jutzi, D. Scheschkewitz, *Angew. Chem. Int. Ed.* **2012**, *51*, 6785 – 6788; *Angew. Chem.* **2012**, *124*, 6891 – 6895.

[27] M. Tang, C. Z. Wang, W. C. Lu, K. M. Ho, *Phys. Rev. B* **2006**, *74*, 195413.

[28] a) F. Furche, R. Ahlrichs, C. Hättig, W. Klopper, M. Sierka, F. Weigend, *WIREs Comput. Mol. Sci.* **2014**, *4*, 91 – 100; b) F. Weigend, R. Ahlrichs, *Phys. Chem. Chem. Phys.* **2005**, *7*, 3297 – 3305.

[29] Experimental details including those on the X-ray diffraction studies of **13**, **14**·$Li^+(thf)_3$, **14**[$Li^+(dme)_3$], and **16** are supplied in the Supporting Information. CCDC 1416161, 1864732, 1864732, and 1864733 (**13**, **14**·$Li^+(thf)_3$, **14**[$Li^+(dme)_3$], and **16**) contain the supplementary crystallographic data for this paper. These data can be obtained free of charge from The Cambridge Crystallographic Data Centre.

[30] a) R. S. Archibald, Y. van den Winkel, A. J. Millevolte, J. M. Desper, R. West, *Organometallics* **1992**, *11*, 3276 – 3281; b) A. Grybat, S. Boomgaarden, W. Saak, H. Marsmann, M. Weidenbruch, *Angew. Chem. Int. Ed.* **1999**, *38*, 2010 – 2012; *Angew. Chem.* **1999**, *111*, 2161 – 2163; c) N. Wiberg, W. Niedermayer, K. Polborn, *Z. Anorg. Allg. Chem.* **2002**, *628*, 1045 – 1052; d) S. Boomgaarden, W. Saak, H. Marsmann, M. Weidenbruch, *Z. Anorg. Allg. Chem.* **2002**, *628*, 1745 – 1748; e) N. Akasaka, K. Fujieda, E. Garoni, K. Kamada, H. Matsui, M. Nakano, T. Iwamoto, *Organometallics* **2018**, *37*, 172 – 175.

[31] D. Auer, C. Strohmann, A. V. Arbuznikov, M. Kaupp, *Organometallics* **2003**, *22*, 2442 – 2449.

Manuscript received: October 2, 2018
Revised manuscript received: December 19, 2018
Accepted manuscript online: January 11, 2019
Version of record online: March 8, 2019

